Simulation of FMCW and M-Sequence Ground Penetrating Radar Systems

Jonathan Platt
Department of Electrical and Computer Engineering
The University of Alabama
Tuscaloosa, AL, USA
jtplatt@crimson.ua.edu
(205) 348-6351

Yang-Ki Hong
Department of Electrical and Computer Engineering
The University of Alabama
Tuscaloosa, AL, USA
ykhong@eng.ua.edu
(205) 348-7268

Hoyun Won
Department of Electrical and Computer Engineering
The University of Alabama
Tuscaloosa, AL, USA
hwon@crimson.ua.edu
(205) 348-6351

Olakunle Olaniyan
Department of Electrical and Computer Engineering
The University of Alabama
Tuscaloosa, AL, USA
ooolaniyan@crimson.ua.edu
(205) 348-6351

Minyeong Choi
Department of Electrical and Computer Engineering
The University of Alabama
Tuscaloosa, AL, USA
mchoi11@crimson.ua.edu
(205) 348-6351

Joohan Lee
Department of Future Technology Convergence
Korea Polar Research Institute
Incheon, South Korea
joohan@kopri.re.kr
(032) 770-6641

2022 IEEE Radio and Wireless Symposium (RWS) | 978-1-6654-3462-1/22/$31.00 ©2022 IEEE | DOI: 10.1109/RWS53089.2022.9719932

***Abstract*— This paper compares the usage of frequency modulated-continuous wave (FMCW) and m-sequence modulation in a ground-penetrating radar scenario. The two radars share a common front-end operating in the 1 to 2 GHz band with a 0 dBm transmitter and a receiver with a noise floor of -60 dBm. The two methods are compared based on their resolution and maximum detectable range. These parameters are examined considering one, four, and ten responses averaged for approximating the impulse response and target range. The simulation results show that even though the FMCW ground penetrating radar (GPR) offers two times higher resolution and maximum detectable range for a single response, the m-sequence GPR becomes superior when considering the average of 10 responses.**

***Keywords*— FMCW, GPR, m-sequence, Radar**

I. Introduction

Ground-penetrating radar (GPR) has the capability of detecting and localizing buried objects. Recently, much attention has been given to the use of ultrawideband (UWB) radars, especially in subsurface sensing GPR applications, due to lightweight, low power consumption and handling, and high resolution of UWB radars [1].

Various modulation methods, such as frequency modulated-continuous wave (FMCW), m-sequence modulation, etc, are reported for UWB GPR systems [1-5]. In particular, the effect of modulation schemes on radar system performance has recently begun to be considered [4-5]. Islam et al. proposed a simulation model for a GPR using FMCW modulation and investigated its achievable range resolution [4]. Robens et al. proposed a simulation model for radar using m-sequence modulation and investigated the effect of noise figures on range accuracy [5]. However, each investigation was limited to a single modulation scheme, and neither attempted to quantify the performance. Accordingly, there is a lack of studies comparing the effect of modulation schemes on GPR resolution and maximum penetration depth.

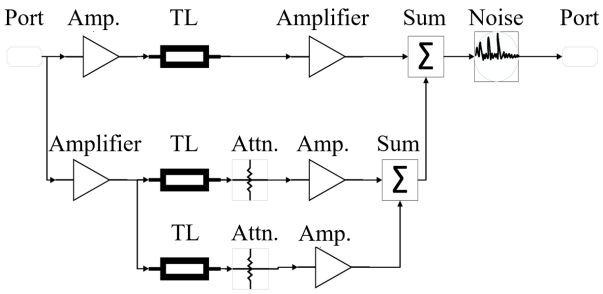

Fig. 1. Buried target simulation model used for both radar systems.

Thus, this paper investigates both FMCW and m-sequence modulations for comparison of GPR performance. Resolution and maximum penetration depth are simulated. The averaging of results over multiple chirp periods for both systems is also considered. Keysight Advanced Design System 2020 Update 1 is used to simulate the GPR systems with the circuit envelop simulator for the RF signals and the Ptolemy simulator for numerical data manipulation in the m-sequence system.

II. Methods

A. *Measurement Scenario*

A set of common measurement scenarios is first established to compare performance between FMCW and m-sequence modulation GPR systems. Considering a drone-mounted UWB GPR system, a simulation model was developed to investigate free space losses between the radar and the ground, reflections from the ground, attenuation losses within the ground, and the radar cross-section of a buried target. Fig. 1 shows the schematic of the stationary target model. The two-way range loss and target

This work was supported in part by the National Science Foundation under Grant number 1650564 and the E. A. "Larry" Drummond Endowment at the University of Alabama.

cross-section are modeled using an amplifier with a fractional gain determined by Eq. (1):

$$Gain = A/(4\pi R)^2, \tag{1}$$

where A is the target's radar cross-section, and R is the total target range. As in [4], the attenuation loss within the ground is calculated by an attenuator with the level of attenuation set by Eq. (2):

$$Loss = 17.4R_g\left(\pi f\mu\varepsilon\sqrt{\sqrt{2\pi f\varepsilon + \frac{\sigma^2}{2\pi f\varepsilon}} - 1}\right), \tag{2}$$

where R_g is the target range through the ground, f is the frequency, and μ, ε, and σ are the ground's permeability, permittivity, and conductivity, respectively. Signals reflected from the surface layer are modeled in a two-part process. First, the incoming signal is split into two paths, one for the reflected signal and another for the transmitted signal, passing into the ground. The reflection coefficient Γ of the ground surface is given by Eq. (3),

$$\Gamma = \left(\sqrt{\mu/\varepsilon} - 1\right)/\left(\sqrt{\mu/\varepsilon} + 1\right), \tag{3}$$

and the transmission coefficient (τ) is $\tau = 1+\Gamma$. The propagation losses for the signal reflected from the ground surface are modeled similarly to the target but using the radar Eq. (4) for flat surfaces [1]:

$$Gain = A/(8\pi R_a)^2, \tag{4}$$

where R_a is the above-ground range. Finally, as in [4], transmission lines are used to model the propagation delays resulting from the target range. The above-ground time delay (T_a) is derived using Eq. (5):

$$T_a = 2R_a/c, \tag{5}$$

where c is the speed of light. The underground time delay (T_g) is calculated by Eq. (6):

$$T_g = 2R_g\sqrt{\mu\varepsilon}, \tag{6}$$

Snow is selected as the ground material to acknowledge the increased interest in applying drone-based radar systems in the remote sensing of the arctic regions [3]. The ground parameters were set as: $\mu = \mu_0$, $\varepsilon = 3\varepsilon_0$, and $\sigma = 1e^{-7}$ $m^{-1}\Omega^{-1}$ [6].

B. *RF Front End System*

Both GPR systems share a set of common parameters for the comparison. Both systems' operation frequency (f_{op}) is in the range of 1 GHz to 2 GHz. The output of both systems is bandpass filtered to 1 to 2 GHz and amplified to an output power of 0 dBm. After passing through the ground target, the signal is received using a 1 to 2 GHz band antenna. The signal is amplified to a total of 20 dB before passing into radar-specific signal processing. All measurement scenarios are conducted considering a -60 dBm.

C. *FMCW Modulated Radar*

Fig. 2 shows the schematic for the FMCW radar system. To generate FMCW modulation, a triangular waveform with a period of 1 μs is generated and used as the voltage-controlled oscillator (VCO) input to generate FMCW modulation. The VCO modulates the triangular waveform into a signal that linearly varies its frequency between 1 to 2 GHz with a repetition frequency of 1 MHz. The VCO output is split between the RF front end and the local oscillator port of a mixer using a 10 dB coupler. The output of the RF front end enters the radio frequency port of the mixer, and the beat frequency is output from the mixer's intermediate frequency port. The beat frequency (f_b) is measured and used to derive the target range (R) according to Eq. (7):

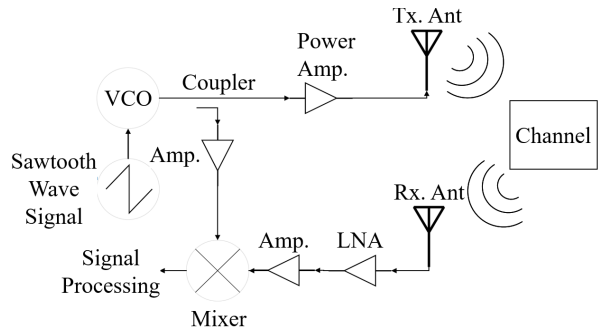

Fig. 2. FMCW radar system block diagram.

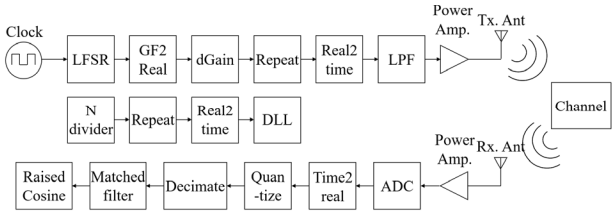

Fig. 3. M-sequence radar system block diagram.

$$R = Cf_b/(4\Delta f \cdot f_m), \tag{7}$$

where Δf is the bandwidth, and f_m is the modulation frequency.

D. *M-Sequence Modulated Radar*

Fig. 3 shows the schematic of the m-sequence system. A linear feedback shift register (LFSR) is configured to generate an order of 10 m-sequence resulting in a period of 1023 chips. Then, the LFSR's binary output (0 and 1) is changed to a sequence consisting of -1 and 1. Each chip is repeated consecutively sixteen times. About 80% of the m-sequence energy is concentrated below one-half of the bandwidth [5]. Since the f_{op} is between 1 and 2 GHz, an RF modulator uses the m-sequence to modulate a 1.5 GHz carrier resulting in a signal with the desired bandwidth. The modulated carrier is then transmitted via Tx antenna to channel.

On the receiving side, the amplified received signal enters an RF demodulator to obtain the baseband m-sequence. An analog-to-digital converter (ADC) samples the baseband signal at the chip rate. The sampled signal is converted back into the numeric domain and quantized according to the resolution of the ADS54RF63 ADC [7]. At this stage, the signal is also down-sampled from 16 samples per chip to one sample per chip. Finally, the processed received signal is cross-correlated with the original m-sequence.

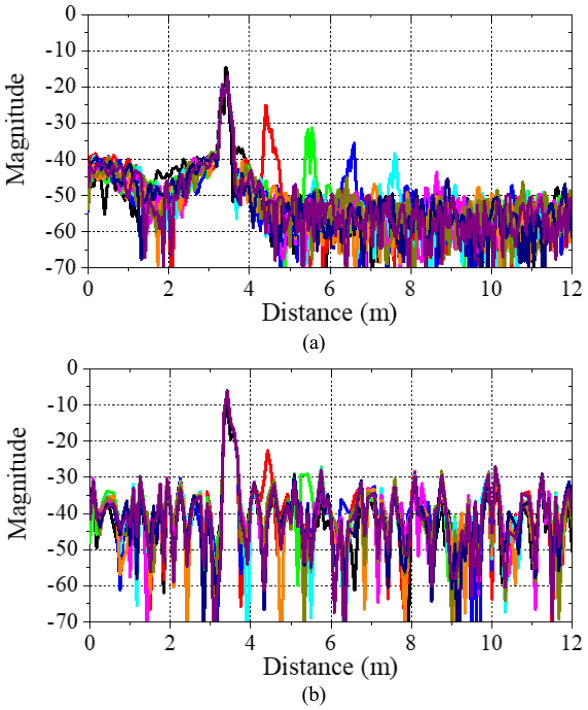

Fig. 4. Received signal of (a) FMCW and (b) M-sequence systems with one average period.

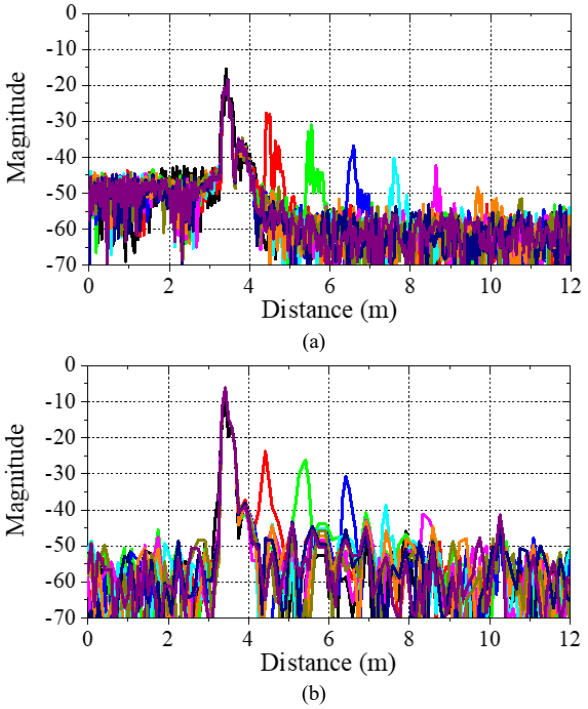

Fig. 5. Received signal of (a) FMCW and (b) M-sequence systems with four average period.

III. Results

The drone-based radar platform is simulated using an above-ground range of 3.4 m to minimize losses while providing sufficient clearance for obstacles. Below the ground, 12 targets are placed parametrically from 0 m depth (at the surface) to 12 m in 1 m increments. The cross-section of the variable depth target is selected as 1 m^2 for simplicity. We considered a single radar return for each scenario and the averaging of 4 and 10 radar returns.

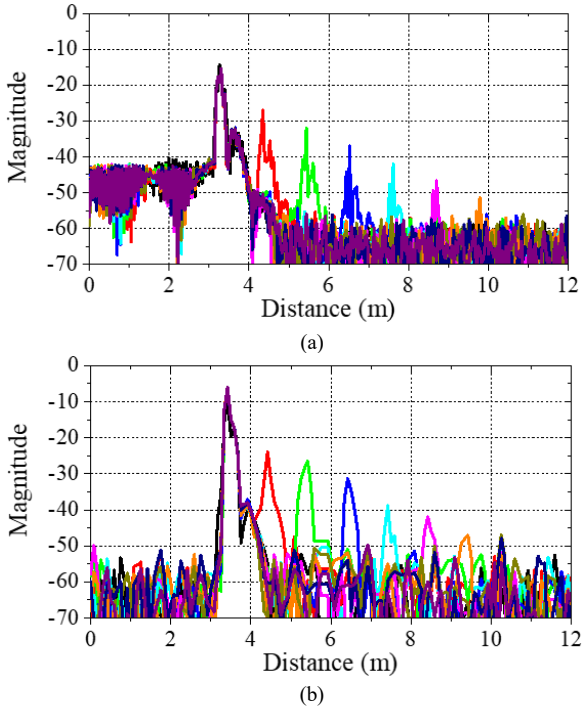

Fig. 6. Received signal of (a) FMCW and (b) M-sequence systems with ten average period.

Fig. 4, 5, and 6 show the received signal of FMCW and m-sequence systems with one, four, and ten average period, respectively. The results show that the resolutions of the FMCW and m-sequence systems are 4.5 and 8.5 cm, respectively, for all averaging periods. For maximum detectable range, at one averaging period, the FMCW GPR can detect up to 5m, while the m-sequence GPR can only detect 2m. At four averaging periods, both GPR systems can detect up to 6m. At ten averaging periods, although the FMCW GPR can detect up to 7 m, the m-sequence GPR can detect up to 8 m. The maximum detectable range was increased up to 11 m for more extended averaging periods. Further, as the averaging period increases, the FMCW GPR suffers from increased clutter, reducing its resolution.

IV. Conclusion

Two ground-penetrating radars (GPRs), employing frequency modulated continuous wave (FMCW) and m-sequence modulations, were described and compared. The results showed that although the FMCW GPR showed higher resolution and maximum range for a single averaging period, the m-sequence GPR surpasses when considering ten averaging periods. Furthermore, the FMCW GPR resolution was reduced as the averaging periods increased, while the m-sequence GPR stayed consistent.

References

[1] R. Jenssen, M. Eckerstorfer, and S. Jacobsen, "Drone-mounted Ultrawideband Radar for Retrieval of Snowpack Properties," *IEEE Trans. Instru. Meas.*, vol. 69, no. 11, pp. 221-230, Jan. 2020.

[2] P. Galajda, M. Pecovsky, J. Gazda, and M. Drutarovsky, "Novel M-sequence UWB Sensor for Groud Penetrating Radar Application," *2018 IEEE APCAP*, Auckland, New Zealand, Aug. 2018.

[3] R. Jenssen and S. Jacobsen, "Drone-mounted UWB Snow Radar: Technical Improvements and Field Results," *J. Electromag. Waves Appl.*, vol 34, no .14, pp. 1930-1954, Mar. 2020.

[4] M. Islam, M. Afzal, M. Ahmad, and T. Tauqeer, "Simulation and Modeling of Ground Penetrating RADARS," *2012 Int. Conf. Emerg. Techn.*, Islamabad, Pakistan, Oct. 2012.

[5] M. Robens, R. Wunderlich, S. Heinen, and J. Sachs, "System simulation for M-sequence radar sensors," *2012 IPIN*, Sydney, Australia, Nov. 2012.

[6] X. Liu, K. Yan, Z. Chen, C. Li, J. Zhang, S. Ye, and G. Fang, "A m-sequence UWB radar system design and contrast test with an impulse radar," *2018 17th Int. Conf. GPR*, Rapperswil, Switzerland, Jun. 2018.

[7] Texas Instruments, "12-bit, 500-/550-MSPS Analog-to-Digital Converters," ADS5463/ADS54RF63 datasheet, Jul. 2009.